Numerical Computation for a Flow Caused by a High-speed Traveling Train and a Stationary Overpass

Shotaro HAMATO[1], Masashi YAMAKAWA[1], Yongmann M. Chung[2], and Shinichi ASAO[3]

[1] Kyoto Institute of Technology, Matsugasaki, Sakyo-ku, Kyoto 606-8585, Japan
Hamato0820@icloud.com
[2] University of Warwick, Gibbet Hill Road, Coventry CV4-7AL, United Kingdom
[3] Collage of Industrial Technology, Amagasaki, Hyogo 661-0047, Japan

Abstract. In the United Kingdom, old infrastructure facilities along train tracks like overpasses should be repaired as soon as possible. In order to design them more optimally, we need to know the flow field around such facilities. In this study, a traveling train and a stationary overpass were reproduced in a computational domain, and the flow field around the train and the overpass was simulated with the MCD method and the Expanded Sliding Mesh approach. In the conventional Sliding Mesh approach, sliding planes must be completely adjacent to other Sliding planes, that is, Sliding planes cannot be adjacent to both other Sliding planes and outer boundaries simultaneously. Then, the Expanded Sliding Mesh approach was proposed. The results given by using the MCD method and the Expanded Sliding Mesh approach were compared with the experimental results given by Baker, and their good qualitative and quantitative agreements were shown in almost cases. Only in the case that the overpass is very close to the train, the effects of boundary layers on laminar flow and turbulence need to be considered for more precise computation.

Keywords: Computational Fluid Dynamics · Compressible Flow · Unstructured Mesh · Moving Grid · High-speed Train

1 Introduction

Railway systems and trains contribute cultural and economical prosperity of cities and nations in the world. In Japan, liner motor trains which are faster than Shinkansen trains by using electrical magnet are about to use. On the other hand, the United Kingdom is the first country which starts to use railway systems. Underground was also developed and used first in the UK. However, the railway systems in the UK are older than those in any other countries, and it should be repaired or rebuild as soon as possible.[1, 2] When such facilities along train tracks would be repaired, these two points should be considered:

1. Repair and rebuilding should be as cheap as possible.

ICCS Camera Ready Version 2020
To cite this paper please use the final published version:
DOI: 10.1007/978-3-030-50417-5_12

2. New one is more difficult to be damaged.

Since the passage of trains is generally related to damage of facilities along tracks, it is necessary to know the flow fields and the pressure distribution around the overpass. A previous research regarding to this problem was reported by Baker[3], which was using an experimental model in 1/25 scale. However, the Baker's experiment is for obtaining data to renew Euro Code for the UK, is not for knowing the flow fields in detail.

We focused on overpasses. Overpasses are a kind of bridges for pedestrians and cars, which are fixed over train tracks. They are commonly used in countries with many plains like the UK and are necessary in people's lives. Therefore, the objectives of this study are expressing a traveling train and an overpass in computer, estimating pressure distribution on the overpass and revealing the flow fields around the traveling train and the overpass in detail. The feature of this study is that the traveling train and the stationary overpass are considered at the same time. In order to achieve the computation with objects which have different motion, the approach combining the MCD method and the Sliding Mesh approach is adopted. A previous research using the approach[4] is already reported, which showed the exactness of computation with large movement of objects or deformation of grid. In this study, the Expanded boundary conditions and the combined approach enable the computation.

2 Numerical Approach

2.1 Govening Equations

In this study, the computations are carried out within inviscid approximation to simplify calculations and shorten the calculation time. The three dimensional Euler equations for compressible flow in conservation form are used as governing equations,

$$\frac{\partial \boldsymbol{q}}{\partial t} + \frac{\partial \boldsymbol{E}}{\partial x} + \frac{\partial \boldsymbol{F}}{\partial y} + \frac{\partial \boldsymbol{G}}{\partial z} = 0 \tag{1}$$

$$\boldsymbol{q} = \begin{bmatrix} \rho \\ \rho u \\ \rho v \\ \rho w \\ e \end{bmatrix}, \boldsymbol{E} = \begin{bmatrix} \rho u \\ \rho u^2 + p \\ \rho uv \\ \rho uw \\ u(e+p) \end{bmatrix}, \boldsymbol{F} = \begin{bmatrix} \rho v \\ \rho uv \\ \rho v^2 + p \\ \rho vw \\ v(e+p) \end{bmatrix}, \boldsymbol{G} = \begin{bmatrix} \rho w \\ \rho uw \\ \rho vw \\ \rho w^2 + p \\ w(e+p) \end{bmatrix} \tag{2}$$

where $\boldsymbol{q}$ is conserved physical quantities, ρ is density and e is total energy per unit volume. Moreover, $\boldsymbol{E}, \boldsymbol{F}, \boldsymbol{G}$ are the inviscid flux functions and u, v, w are velocity components for x, y, z axes respectively. Equation of State for a Perfect gas is used to obtain pressure,

$$p = (\gamma - 1)\left\{ e - \frac{1}{2}\rho\left(u^2 + v^2 + w^2\right)\right\} \tag{3}$$

where γ is the specific heat ratio and $\gamma = 1.4$ in this study.

ICCS Camera Ready Version 2020
To cite this paper please use the final published version:
DOI: 10.1007/978-3-030-50417-5_12

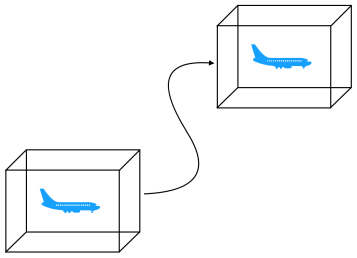

Fig. 1. Conceptual image of the MCD method

The Roe's Flux Splitting method is used for evaluating the inviscid flux functions. Physical quantities are defined at each cell center. For higher-ordering, the MUSCL method with the Venkatakrishnan's limiter is adopted. The Rational Runge-Kutta method is employed for time integration in pseudo-time steps.

2.2 MCD Method

Computation including movement and deformation of bodies is called the moving boundary problem in general. In order to solve such problems, the whole movement path and the deformation range of the bodies should be included in a computational domain. Thus, the massive computational domain is needed, and such computation will take much time and computational cost.

The MCD method (Moving Computational Domain method)[5–7], which is a kind of Finite volume method for Unstructured moving grid[8, 9], has been proposed for the moving boundary problem and was adopted in this study. In the MCD method, the whole computational grid is moved according to the bodies to express the movement of bodies. The main good point of the MCD method is that there is no restriction of movement. The bodies can move in infinite domain without restriction of its movement. Moreover, computational cost will be saved because computational domain do not need to include all of the movement pass and can be smaller than in conventional method. Since the four-dimensional volume in a space-time unified domain is used as control volume, the Geometric Conservation Law (GCL)[10] and the physical conservation law are satisfied automatically and exactly. Many previous researches of Racing car[11] or Tilt-Rotor plane[12] using the MCD method have been already reported. In this study, the computation of the stationary overpass and the traveling train was carried out by a new method combining the MCD method and the Expan

2.3 Sliding Mesh Approach

The moving boundary problem can be solved just by the MCD method. If the overpass and the train were included in the same computational domain, the

ICCS Camera Ready Version 2020
To cite this paper please use the final published version:
DOI: 10.1007/978-3-030-50417-5_12

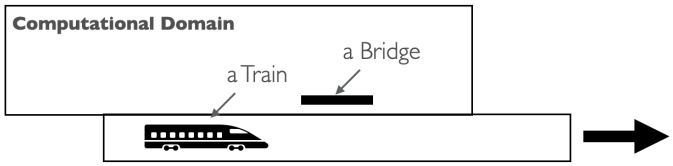

Fig. 2. Conceptual image of the Sliding Mesh approach

overpass would be moved because of the movement of the computational domain to express the movement of the train. Then, the Sliding Mesh approach enables to simulate objects which have different motions. In the Sliding Mesh approach, the computational domain is divided into two or three computational domains, and these domains are facing to each other and slid to express different motions. Physical quantities are interpolated and communicated between these domains while sliding. The interpolation method is introduced in detail below.

Figure 3(a) shows the faces of cells on the dividing plane, which is called the Sliding plane in this paper. The face of the cell i belongs to the computational domain of the train, and the faces of the cells j belong to the computational domain of the overpass. They are adjacent to each other on the Sliding plane, that is, the cell i is adjacent to and overlapping with the cells j. The overlapping areas of the cell i and the cells j are calculated and the interpolated values are based on the each area and the each physical quantity of the cells. The interpolating formula is shown below,

$$\boldsymbol{q}_{bi} = \frac{\sum_{j \in i} \boldsymbol{q}_j S_{ij}}{S_i} \tag{4}$$

where $\boldsymbol{q}_j$ is each physical quantity of cells j, $\boldsymbol{q}_{bi}$ is the physical quantity of the ghost cell of the cell i, S_{ij} is the overlapping areas of the cell i and the cells j and $\sum_{j \in i}$ means the summation of the values of all the cells j which is adjacent to the cell i. Previous researches using the Sliding Mesh approach have been reported. However, in these researches, Sliding planes must be completely adjacent to other Sliding planes, that is, Sliding planes cannot be adjacent to both other Sliding planes and outer boundaries simultaneously. Then, in this study, the boundary condition on Sliding planes is improved and expanded.This Expanded Sliding Mesh approach enables to solve the problem that Sliding planes are adjacent to both other Sliding planes and outer boundaries at the same time.

Figure 3(b) shows that a sliding plane is adjacent to the other sliding plane and outer boundaries simultaneously. The part of the boundary which is adjacent to the other Sliding plane is called the Sliding boundary, and the part of the boundary which is adjacent to the outer boundary is called the Outer-Sliding boundary. At the Sliding boundary, the interpolation of the physical quantities is using the Equation 4. On the other hand, at the Outer-Sliding boundary, the physical quantities are estimated with the MCD method as the complete outer

ICCS Camera Ready Version 2020
To cite this paper please use the final published version:
DOI: 10.1007/978-3-030-50417-5_12

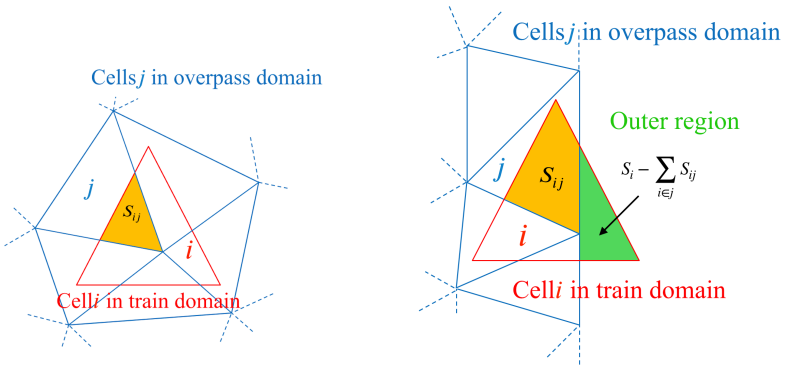

(a) Conventional (b) Expanded

Fig. 3. Relationships of the triangles on sliding planes

boundary at first, and then these quantities are weighted by the outer area and added to the quantities computed by the Equation 4. These computation is formulated as shown below,

$$\boldsymbol{q}_{bi} = \frac{\sum_{j \in i} \boldsymbol{q}_j S_{ij} + \boldsymbol{q}_{oi}(S_i - \sum_{j \in i} S_{ij})}{S_i} \tag{5}$$

where $\boldsymbol{q}_{oi}$ is physical quantities computed by the MCD method as the complete outer boundary.

3 Inspection for Geometric Conservation Law

In this section, the inspection of the approach combining the MCD method and the Expanded Sliding Mesh approach is carried out with a uniform flow problem. Whether the extended boundary condition satisfies the Geometric conservation law is checked.

3.1 Computational Grid

Figure 4 shows the computational grid for the uniform flow problem. The small pink rectangular moves for positive x-axis at velocity 0.1, and the small yellow rectangular moves for negative x-axis at velocity -0.1. Unstructured grid is generated by MEGG3D[13, 14]. The number of elements is 594,794.

3.2 Computational Conditions

All the cells have $\rho = 1.0, p = \frac{1}{\gamma}, u = v = w = 1.0$ as an initial condition. As boundary conditions, initial conditions are remained at outer boundary. The

ICCS Camera Ready Version 2020
To cite this paper please use the final published version:
DOI: 10.1007/978-3-030-50417-5_12

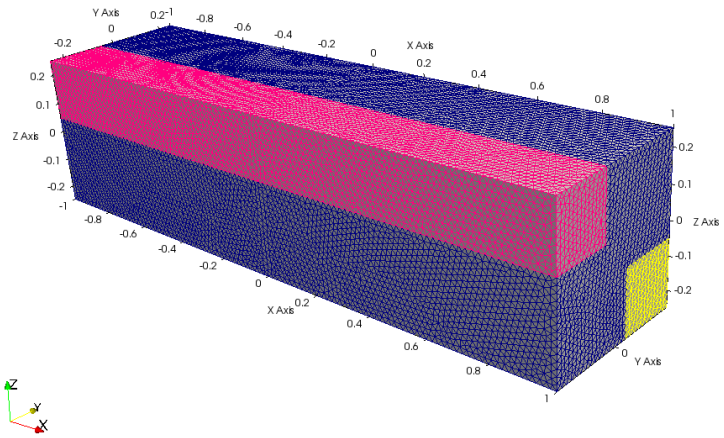

Fig. 4. Computational grid for uniform flow inspection

Sliding boundary condition is applied to the sliding boundary, and the Sliding-Outer boundary condition is applied to the Sliding-Outer boundary. Time width is 0.005 and the computation lasts for dimensionless time 16000.

3.3 Result

Density error is defined by Equation 6. The maximum value of the density errors among all the cells is the density error at each time step.

$$\mathrm{ERROR}_n = \max\left(\frac{|\rho_\infty - \rho_i|}{\rho_\infty}\right) \tag{6}$$

Figure 5 shows the error history of the density errors. The orders of the errors are under 10^{-12}, which is the range of mechanical error. Therefore, it is proved that the MCD method and the Expanded Sliding Mesh approach do not give any effect to the flow fields.

4 Application for a Train and an Overpass

In this section, the computation of the train passing through the stationary overpass is achieved with the MCD method and the Expanded Sliding Mesh approach. Moreover, the numerical results are compared qualitatively and quantitatively with the experimental results carried out by Baker to confirm the validity of the numerical results.

ICCS Camera Ready Version 2020
To cite this paper please use the final published version:
DOI: 10.1007/978-3-030-50417-5_12

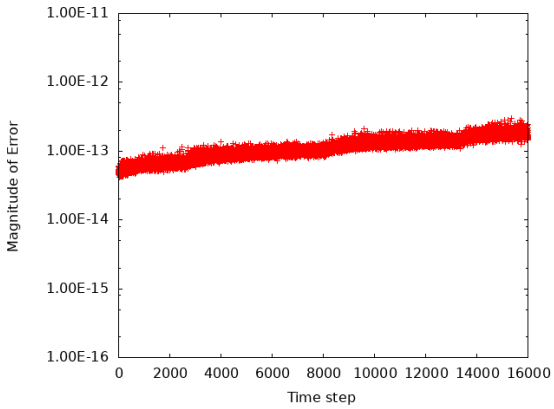

Fig. 5. Density error history

Table 1. Sizes of the experimental model of the Class390 made by Baker[3]

[m]	Real scale	1/25 scale
Length	37.35	1.48
Width	2.73	0.11
Height	3.56	0.14

4.1 Introduction of Previous Research

First, the previous experiment carried out by Baker is explained for comparing. The Baker's experiment was carried out in order to obtain a fundamental understanding of the nature of aerodynamical phenomena caused by the passages of trains and to obtain data for a variety of railway infrastructure geometries of particular relevance to the UK situation.

Experimental model In the experiment, 4 types of trains and 3 types of trackside facilities were adopted. In particular, the Class390 and the overpass are explained here.

First, the Class390is the common train in the UK, which has streamline of the head carriage and the notch on the ceiling. Baker made the experimental model of the Class390 in 1/25 scale(See Fig 6(a)). The sizes of the Class390 in real scale and in 1/25 scale are shown in Tab 1.

Next, as explained in Section1, overpasses are a kind of bridges for pedestrians and cars, which are fixed over train tracks. Baker made the experimental model of the overpass with an elastic plate in 1/25 scale and it is fixed over the train track with the piers, shown in Fig 6(b). The sizes of the overpass in real scale and 1/25 scale are shown in Fig 2.

ICCS Camera Ready Version 2020
To cite this paper please use the final published version:
DOI: 10.1007/978-3-030-50417-5_12

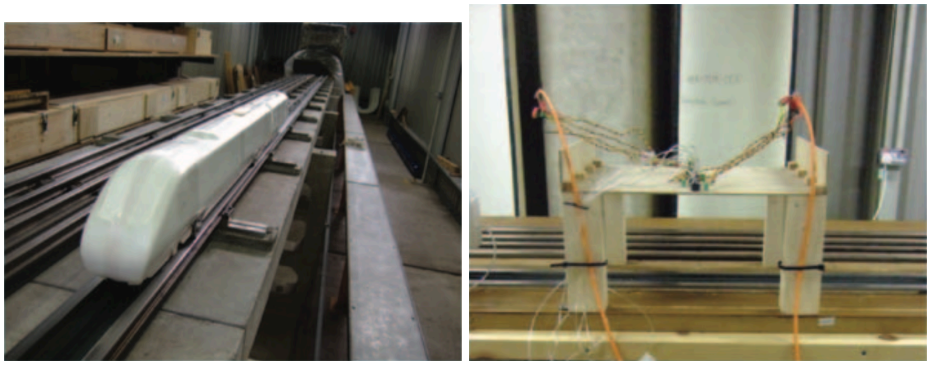

(a) Train(Class390) (b) Overpass

Fig. 6. Experimental models made by Baker[3]

Table 2. Sizes of the experimental model of the overpass made by Baker[3]

[m]	Real scale	1/25 scale
Width	10.0	0.4
Length	5.0	0.2
Height Case1	4.5	0.18
Case2	5.0	0.2
Case3	5.5	0.22
Case4	6.0	0.24

Experimental condition The measurement points of pressure are explained here. The lower surface of the overpass is shown in Fig 7. The sensors for pressure measurement are set at the stars. The sensors are set every 1.0m in real scale (every 40mm in 1/25 scale), they are set symmetrically for the center line of the overpass.

4.2 Evaluation of Pressure

An evaluation method for pressure measured on the lower surface of the overpass is explained in this section. In the Baker's experiment, all the results of pressure were evaluated as pressure coefficients using the Equation 7. For comparing, our results will be evaluated as pressure coefficients using the same equation.

$$C_{\mathrm{p}} = \frac{p - p_{\infty}}{\frac{1}{2}\rho_{\infty}U^2} \tag{7}$$

where p is pressure measured at the each measurement point on the lower surface of the overpass, ρ_{∞} and p_{∞} is constant density and constant pressure respectively, and U is the traveling speed of the train.

ICCS Camera Ready Version 2020
To cite this paper please use the final published version:
DOI: 10.1007/978-3-030-50417-5_12

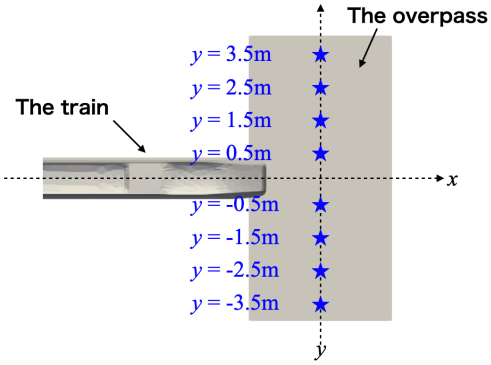

Fig. 7. Pressure measurement points on the overpass model

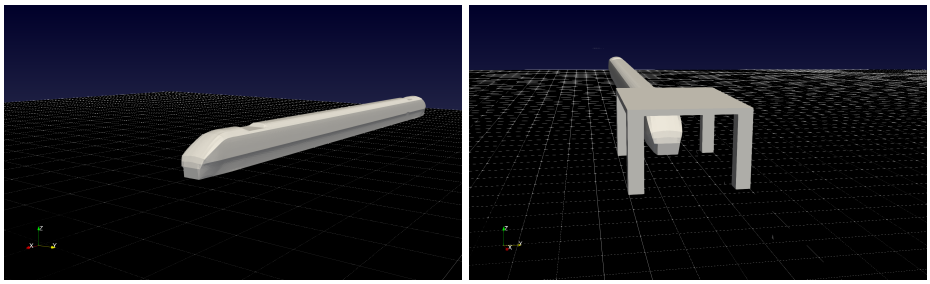

(a) Train(Class390) (b) Overpass

Fig. 8. Computational model

4.3 Computation of the traveling train under the overpass with the piers

First, the computations that the height of the overpass is 5.5m and 6.0m are carried out in order to check the validity of the code and the results qualitatively. After that, the computations that the overpass is very close to the traveling train (the height of the overpass is 4.5m and 5.0m) are carried out in order to obtain a variety of the results.

Computational model and conditions The numerical models are shown in Fig 8, the computational grid is shown in Fig 9, and the overview and the sizes of the computational domains are shown in Fig 10. The shape of the numerical models of the train and the overpass are almost the same with the experimental models. The streamline of the head carriage and the notch shape on the ceiling are reproduced. The overpass is modeled as rigid plate. The computational grid is generated by MEGG3D.

ICCS Camera Ready Version 2020
To cite this paper please use the final published version:
DOI: 10.1007/978-3-030-50417-5_12

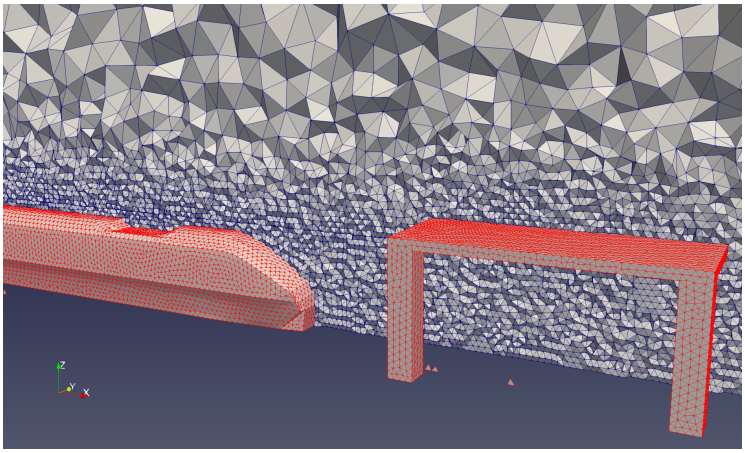

Fig. 9. Computational grid

Computation of the wider gap cases At first, the results of the cases that the height of the overpass is 5.5m and 6.0m are shown and discussed. These cases are called "the wider gap cases" below. Pressure distribution on the lower surface of the overpass in the wider gap cases at dimennsionless time t=45 and 56 is shown in Fig 11. The range of the color bars is set at the same. At both time steps, pressure is higher and lower at height=5.5m than at height=6.0m, that is, pressure changes more dynamically in the case that the overpass is close to the train. It means pressure fluctuation depends on the height of the overpass. Moreover, such aerodynamical phenomenon is expressed by numerical simulation.

Difference between the maximum and the minimum pressure coefficients in the wider gap cases obtained by Baker and our numerical computation is plotted in the Fig 12. Pressure coefficients are calculated as explained in the Section 4.2. As shown in Fig 12, the experimental results and the numerical results have almost the same distribution. Thus, the qualitative and quantitative agreements of them are proved in the wider gap cases.

Computation of the narrower gap cases Next, the results of the cases that the height of the overpass is 4.5m and 5.0m are shown and discussed in this subsection. These cases are called "the narrower gap cases" below. Pressure distribution on the lower surface of the overpass in the narrower gap cases at dimensionless time t=45 and 56 is shown in Fig 13. As in the previous subsection, pressure changes more dynamically in the case that the overpass is close to the train. It is shown that the height of the overpass affects dynamical pressure fluctuation not only in the wider cases but also in the narrower cases.

Difference of the maximum and the minimum pressure coefficients in the narrower cases obtained by the Baker's experiment and the our numerical computation is plotted in Fig 14. The basic tendency of pressure distribution, which

ICCS Camera Ready Version 2020
To cite this paper please use the final published version:
DOI: 10.1007/978-3-030-50417-5_12

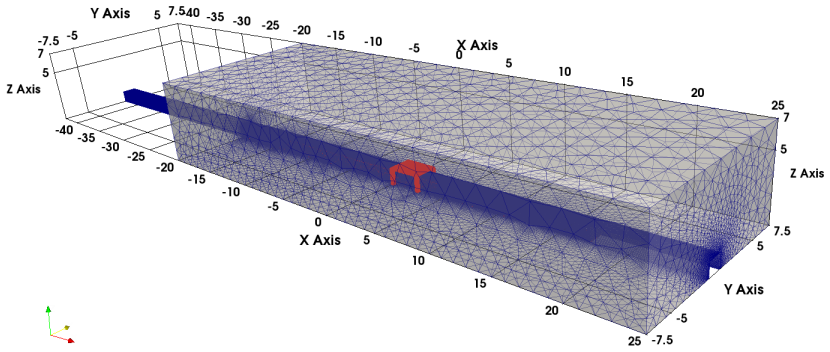

Fig. 10. Sizes of Computational grid

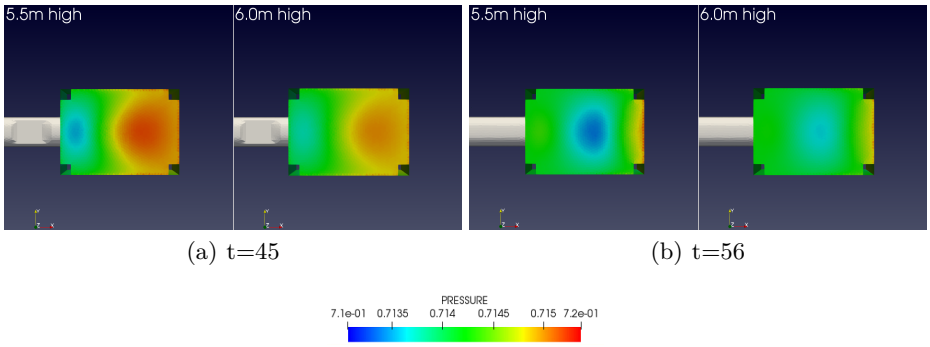

(a) t=45 (b) t=56

Fig. 11. Pressure distribution on the lower surface of the overpass (the wider gap cases)

is symmetrical at the center line (y=0), is almost expressed also in the narrower cases. Therefore, the qualitative agreements are proved.

However, there are some quantitative disagreements in the narrower cases. First, pressure coefficients around the both ends (y=-3.5m and 3.5m) of the numerical results in Fig 14 are overpredicted. Second, the maximum pressure coefficients of the numerical results are quite different from those of the experimental results. The error of the maximum pressure coefficients is about 23%.

The reasons why these differences occurred are discussed below. Ignoring viscosity and boundary layers would be one possibility. Actual fluids have viscosity. Boundary layers are appeared along the wall of moving bodies and the layers give influences to the flow fields. In our study, since it is supposed that the fluid is inviscid, the influence of the boundary layers to the flow fields is completely ignored. In the situation that the train is very close to the overpass, the influence should be considered because the gap between the train and the

ICCS Camera Ready Version 2020
To cite this paper please use the final published version:
DOI: 10.1007/978-3-030-50417-5_12

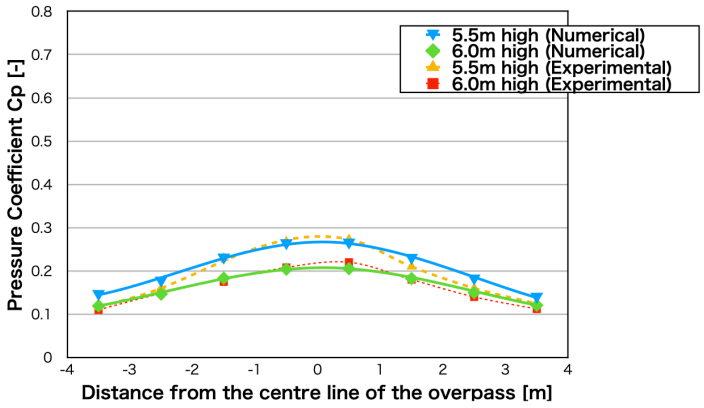

Fig. 12. The lateral peak-to-peak distribution on the lower surface of the overpass (the wider gap cases)

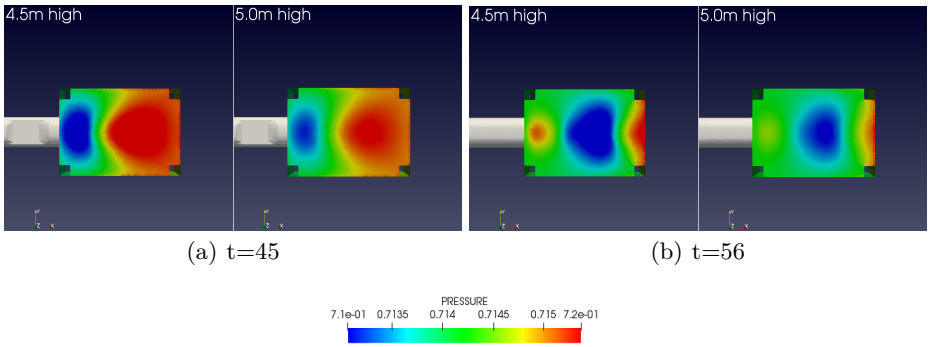

(a) t=45 (b) t=56

Fig. 13. Pressure distribution on the lower surface of the overpass (the narrower gap cases)

overpass is small. The order of the boundary layer based on the Prandtl's Laminar Boundary layer Equation is 1.77×10^{-3}, which is about 1% towards the gap. The boundary layer will be bigger in turbulence, and the influence of the turbulent and laminar boundary layer will be more significant. If the physical quantities in the flow fields like pressure or velocity are altered with the influence of the layers in laminar flow and turbulence, the numerical results may agree with the experimental results.

Now we have developed the numerical simulation code for viscous flow with the numerical model of the train and the overpass.

ICCS Camera Ready Version 2020
To cite this paper please use the final published version:
DOI: 10.1007/978-3-030-50417-5_12

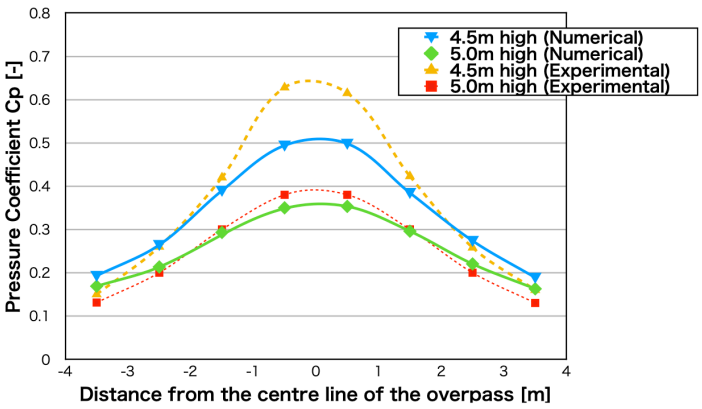

Fig. 14. The lateral peak-to-peak distribution on the lower surface of the overpass (the narrower gap cases)

5 Conclusions

The objective of this study is to simulate the flow fields driven by the train passage and to estimate the effects of them like pressure wave in order to help optimal reconstruction and rebuild of old overpasses, which are often seen in the UK. The new method combined the MCD method and the Expanded Sliding Mesh approach was proposed and had been shown to satisfy the geometric conservation law. Using the new method, the numerical simulations of the four cases which had different height of the overpass were conducted within the inviscid approximation. In the cases of the wider gap that the height of the overpass is 5.5m and 6.0m, the numerical results agreed almost completely with the experimental results. Therefore, it was shown to be able to reproduce the flow field around the traveling train and the overpass in computer and fully estimate pressures acting on the lower surface of the overpass even within the inviscid approximation. However, in the cases of the narrower gap that the height of the overpass is 4.5m and 5.0m, the pressure fluctuation of the results of the numerical simulation was under-estimated. The one of the reasons of the disagreement would be the inviscid approximation. In the real world, the flow field around the traveling train and the overpass is under the influence of laminar or turbulent boundary layer in the case that the train is very close to the overpass. But in this computation, such influences were ignored at all. Now, we have been developing the simulation code for the viscous compressible flow and computations are now running.

In the case that there is appropriate distance between the train and facilities like overpasses, it was shown to be able to estimate the effect of train passages to the facilities even within the inviscid approximation. This method combined the MCD method and the Expanded Sliding Mesh approach can be applied to computations including another facilities, for instance station platforms, or other

ICCS Camera Ready Version 2020
To cite this paper please use the final published version:
DOI: 10.1007/978-3-030-50417-5_12

kind of trains and also could help old facilities be reconstructed and rebuild. More accurate and detailed flow simulation considering viscosity will be required in the further study.

6 Acknowledgments

This publication was subsidized by JKA through its promotion funds from KEIRIN RACE.

References

1. Hori, M.: A study on railway reform in Britain. From the viewpoint of structural separation(Translated from Japanese). Tourism Studies Vol.8 (2009), p.57
2. Koyakumaru, S.: Recognition of reforms and new developments in British Railways(Translated from Japanese). Transportation and Economy Vol.72 No.7 (2012), p.74
3. Baker, C., et al.: Transient aerodynamic pressures and forces on trackside and overhead structures due to passing trains. part 1: Model-scale experiment part 2: Standards applications. Journal of Rail and Rapid Transit, Vol.228(1) (2014), pp.37-70
4. Takii, A., et al.: Six degrees of freedom numerical simulation of tilt-rotor plane. ICCS2019, LNCS1153 (2019), pp.508-510
5. Yamakawa, M., Mitsunari, N., et al.: Numerical simulation of rotation of intermeshing rotors using added and eliminated mesh method. Proc. Comput. Sci. 108 (2017), pp.1183-1192
6. Asao, S., et al.: Simulations of a falling sphere with concentration in an infinite long pipe using a new moving mesh system. Appl. Therm. Eng. 72 (2014), pp.29-33
7. Asao, S., et al.: Parallel computations of incompressible flow around falling spheres in a long pipe using moving computational domain method. Comput. Fluids 88 (2013), pp.850-856
8. Yamakawa, M., Matsuno, K., et al.: Unstructured moving-grid finite-volume method for unsteady shocked flows. J. Comput. Fluids Eng. 10-1 (2005), pp.24-30
9. Yamakawa, M., Takekawa, D., Matsuno, K., et al.: Numerical simulation for a flow around a body ejection using an axisymmetric unstructured moving grid method. Comput. Therm. Sci. 4(3) (2012), pp.217-223
10. Obayashi, S., et al.: Free-stream capturing for moving coordinates in three dimensions. AAIA J. 30 (1992), pp.1125-1128
11. Watanabe, K., Matsuno, K., et al.: Moving computational domain method and its application to flow around a high-speed car passing through a hairpin curve. J. Comput. Sci. Technol. 3(2) (2009), pp.449-459
12. Yamakawa, M., Chikaguchi, S., Asao, S.: Numerical simulation of tilt-rotor plane using multi axes sliding mesh approach. The 27th International Symposium on Transport Phenomena, Honolulu (2016)
13. Ito, Y.: Challenges in unstructured mesh generation for practical and efficient computational fluid dynamics simulations. Comput. Fluids 85 (2013), pp.47-52
14. Ito, Y., Nakanishi, K.: Surface triangulation for polygonal models based on cad data. Intern. J. Numer. Methods Fluids 39(1) (2002), pp.75-96

ICCS Camera Ready Version 2020
To cite this paper please use the final published version:
DOI: 10.1007/978-3-030-50417-5_12